Scientific Research Publishing

International Journal of Organic Chemistry, 2023, 13, 57-85
https://www.scirp.org/journal/ijoc
ISSN Online: 2161-4695
ISSN Print: 2161-4687

Hirshfeld Surface Analysis for Investigation of Intermolecular Interaction of Molecular Crystals

Shintaro Suda, Atsunobu Tateno, Daisuke Nakane, Takashiro Akitsu*

Department of Chemistry, Faculty of Science, Tokyo University of Science, Tokyo, Japan
Email: *akitsu2@rs.tus.ac.jp

How to cite this paper: Suda, S., Tateno, A., Nakane, D. and Akitsu, T. (2023) Hirshfeld Surface Analysis for Investigation of Intermolecular Interaction of Molecular Crystals. *International Journal of Organic Chemistry*, **13**, 57-85.
https://doi.org/10.4236/ijoc.2023.132006

Received: April 22, 2023
Accepted: June 13, 2023
Published: June 16, 2023

Abstract

Hirshfeld surface analysis has been widely used in recent years as a means to quantify and visualize various types of intermolecular interactions in molecular crystals. This review article introduces intermolecular interactions discussed with Hirshfeld surface analysis and 2D fingerprint plots. In addition, using CIF files obtained from our previous results, Hirshfeld surface analysis was newly performed, and the resulting 3DHirshfeld surfaces, 2D print plots, molecular structural features, and crystal structure relationships were described. Classification of their intermolecular interactions, statistical discussion focused on crystalline water and perspective on ligand-protein docking are also mentioned.

Keywords

Chemical Crystallography, Cambridge Structure Database, CIF, Hirshfeld Surface Analysis, Schiff Base

1. Introduction

Intermolecular interactions in molecular crystals are important not only for forming crystal packing but also for molecular recognition and supramolecular formation [1]. Conventionally, specific intermolecular interactions have often been pointed out by observing crystal structure analysis results. In recent years, by inputting the crystal structure, it has become possible to theoretically and visually quickly analyze the length of the interatomic distance, the donor/acceptor atoms, and the contribution rate. Nowadays, Hirshfeld surface analysis can be performed by loading CIF files obtained from crystal structure analysis into available programs, whose key features may be visualization and quantitation of

various types of intermolecular interactions. Recently, many papers published in MDPI's journals have used Hirshfeld surface analysis to discuss various types of intermolecular interactions [2]-[41].

First, we give typical examples, including weak ones, of basic hydrogen bonding, based on the difference in electronegativity between the donor and acceptor atoms. Zeng *et al*. predominantly explained O-H···O hydrogen bonds and other types of weak interactions in molecular crystal [2]. Kumar *et al*. analyzed the interatomic (O···H, H···H, and C···O) interactions that significantly influence crystal packing for monomer and trimer 5-Hydroxymethyluracil [3]. Semenova *et al*. applied eight coordinated Dy(III) complexes to chiral molecules and mentioned that this association might be due to the O-H···O bonding of aqua ligands, which is denied by long O···O separations [4].

It should be noted that the case of atoms that are weak in terms of electronegativity, such as between carbon atoms and hydrogen atoms, are also introduced here. Bojarska *et al*. carried out in silico research on oligopeptides in O···H/H···O and C···H/H···C interactions [5]. Craciun *et al*. performed analyses of 1D and 2D coordination polymers of Cd(II) complexes with H···H, H···O/O···H, H···C/C···H, H···N/N···H, C···O/O···C, C···N/N···C, C···C, and O···O contacts [6]. Deeloed *et al*. confirmed that the primary interaction between packed complex cations and nitrate anions in the crystal of Ni(II) complexes are H···O/O···H, H···H, and H···N/N···H hydrogen bonds [7]. Gacki *et al*. explained crystal-packing arrangements defined by three (H···H, C···H, and O···H) contacts for quasi-isostructural Co(II) and Ni(II) complexes [6]. Krupka *et al*. examined the contribution of different types of H···H, C···C, O···H/H···O, C···H/H···C interactions to salen-type com-pounds [8]. Mahmoudi *et al*. observed that crystal packing of novel Pb(II) complexes is dominated by C-H···O/N/S interactions [9].

Although it is possible to make a judgment by the usual method based on the observation of the crystal structure, there are also analytical reports on the types of hydrogen bonds involving halogen atoms with strong polarity and sulfur atoms with large polarization. Noor observed intermolecular C-H···Br hydrogen bonding in halide-containing mono(aminopyridine) Fe(II) complexes [10]. Masternak *et al*. suggested the importance of H···F/F···H close contacts in Cu complex cations and SiF_6^{2-} or BF_4^- counterions [11]. Altowyan *et al*. discussed short contacts of N···H, S···H, C···C, and S···C interactions to form crystals of compounds with indolyl-triazole-thiadiazole heterocyclic rings [12]. Ghazzy *et al*. discussed O···H/H···O, C···O/H···C, O···S/S···O, O···O; C···C, H···H, S···S, and C···H interactions of S-containing ferrocene derivatives [13]. Altowyan *et al*. detected short H···H, N···H, S···H, and Cl···H interactions in a Cu(II)-thiazolidine complex [14]. It should be noted that Seth found Cu···O/O···Cu contacts based on the fingerprint of Cu coordination polymers for interaction between metal-negative charged polar atom [15].

Similar to hydrogen bonding, negatively polarized π-systems, or between π-systems, may also participate in intermolecular interactions. Since the phenyl group has a flat plate shape, the aspect of recognizing the three-dimensional shape

becomes stronger, in other words, stacking. Baykoc *et al*. also performed a database survey of relevant (oxadia-zole)···π interactions in both the Cambridge Structural Database and the Protein Data Bank [16]. Jmai *et al*. distinguished various types of interactions, such as van der Waals forces, hydrogen bonds, and C-H···π, and N-H···π interactions for the histaminium bis(Trioxonitrate) compound [17]. Zamisa *et al*. showed that weak intermolecular C-H···O, C-H···N, and C-H···π hydrogen bonds were observed in the crystal lattice of 2-Formimidate-3-carbonitrile compounds [18]. Interactions between π-systems are often weaker than those between polarized atoms. Sukhikh *et al*. identified weak π-π interactions between phthalocyanine metal complexes [19]. Novoa-Ramírez *et al*. showed that π···π interactions in compound Nisalphen stabilized the formation of the dimeric structures of Schiff base Ni(II) complexes [20]. Asad *et al*. observed an indication of the presence of aromatic stacking, as well as H···H, H···O, C···H, C···C, and C···O interactions in piperidinium dicoumarol reprted [21].

Electrostatic attraction dominates when negatively or positively charged atoms participate in hydrogen bonding due to deprotonation or protonation, or when there is a positive or negative ionic component of an ionic crystal. In some cases, polarized atoms and hydrogen atoms form hydrogen bonds at the same time. The counterion of the ionic crystal becomes an element of the supramolecular crystal structure. Minaeva *et al*. investigated NH···Cl, CH···Cl, and CH···O intermolecular interactions and the resulting formation of the NH_2^+-Cl^-, *i.e*., the salt of methylone hydrochloride crystals [22]. Ruelas-Álvarez *et al*. reported the formation of N^+-H···-O/O and O-H···-O/O-type interactions in monobrone compounds [23]. Zieba *et al*. indicated a correlation between intermolecular H···O and O···H contacts in N-H···O, C-O-···H, and O-H···O, as well as conductivity in pyrazolium salts [24]. Zhuang *et al*. applied the weakly supramolecular interaction of $[BiCl_4(phen)]^-$ anions [25]. Smarun *et al*. exhibited short N-H···F contact between the H atom and the PF6 anion group in phosphine-imidazolium salt [26].

There are not only electrostatic attractive interactions between different atoms, but also strong covalent interactions between the same atoms. It is common to compare the interatomic distance predicted from the sum of atomic radii and the actual interatomic distance to show that attractive interactions work, but there is an advantage that becomes clearer through analysis. Hydrophobic effects may also need to be considered in the case between hydrogen atoms. Daśko *et al*. found that Cl···X becomes comparable with hydro-phobic H···H plus C···H intermolecular interactions in triazole compounds [27]. Vassilveva *et al*. treated intermolecular (H···H) contacts between crystallographically independent organic cations and negatively charged $\left[Pb_2Cl_6\right]_n^{2n-}$ chains [28]. Boraei *et al*. reported that S···H, N···H, S···C, and C···C contacts are the most significant to dichlorobenzylidene compounds [29]. Collart *et al*. found a notable difference in F···F interactions in lithium bis(pentafluoroethanesulfonyl)imide [30]. Grudova *et al*. found that intermolecular contacts of H···H, C···H, O···H, and F···H involv-

ing hydrogen atoms (not aurophilic interactions Au(I)···Au(I)) have the largest contribution to crystal packing of cation Au(I) complexes [31].

In molecular crystals, intermolecular interactions generally exist in the repeated arrangement of molecules and ions of the same kind. As an application of the knowledge of intermolecular interactions based on crystal structure and three-dimensional structure, it is necessary to consider molecular recognition, not necessarily through the same chemical species, but to design inhibitor molecules by docking between proteins and ligands. Hamlaoui *et al*. revealed major interactions caused by H···H, H···S/S···H, H···C/C···H, C···C and H···N/N···H contacts of Co(II) complexes as potential inhibitors of HIV-1 protease [32]. Shivanna *et al*. observed a major contribution from H···H in 1-(4-(Methoxy(phenyl) methyl)-2-methylphenoxy) butan-2-one as an α-glucosidase inhibitor [33]. Osman *et al*. showed that adamantane-linked 1,2,4-triazole derivatives (potential 11β-HSD1 inhibitor) provide the data of non-covalent H···H interactions, occupying 54.4% [34]. The use of protein crystal structures, theoretical calculations, and computational chemistry of protein-ligand docking deepens our understanding. According to this point of view, the host protein must also consider flexibility and dynamic factors that allow the three-dimensional structure to fluctuate to some extent. Knowledge of intermolecular interactions and supramolecular chemistry in a broad sense, assuming solutions, is also required. Abou-Taleb *et al*. visualized the crystal structure and the most likely (carboxylic O atom) sites for interactions of ketoprofen crystals that support theoretical docking simulations [35].

In order to form small-molecule crystals of molecular and ionic substances that are the subject of chemical crystallography, we should consider not only the stable structure of a single molecule (optimized structure in computational chemistry) but also the deformation due to crystal packing, dominant intermolecular interactions are one of the important crystal structure determinants, such as space group and molecular arrangement. However, the crystal structure is not limited to one, and there may be multiple possibilities represented by polymorphism or phase transition. Even then, it is the intermolecular interactions that bind the building blocks together. Moyano *et al*. rationalized the crystal stabilization of N-O···H-C interactions for dimethylpyrazoles [36]. Wattanathan *et al*.'s Ce(III) complexes suggested that the C-H···O and C-H···π interactions significantly contribute to crystal packing [37]. Zhou *et al*. predicted that O···O contact is predominantly formed in the most stable Pna21 space group for nitryl cyanide [38]. Standish *et al*. found H···O|O···H, H···N|N···H spikes were well established as common motifs within structural fingerprints for polymorphs of a 2,1,3-benzoxadiazole derivative [39]. Rayes *et al*. reported M-X···H contacts in organic-inorganic salts of perhalidometallates, exhibiting single crystal-single crystal transformation [40].

In the analysis, which was proposed in 1977 [41] and recently used to review actual usage in single molecule magnets [42], a space is defined in which the

electron density of the molecule of interest is greater than the surrounding electron density. This space wraps the outer region, similar to a cover, and is called the 'Hirshfeld surface'. The strength of intermolecular interactions is printed on the Hirshfeld surface, which is colored red when the molecules are close to the surrounding atoms and blue when they are far from the surrounding atoms. This yields the visualization of which parts of the crystal structure are interacting and with what strength. Furthermore, whereas van der Waals surfaces defined by known van der Waals radii are only defined by the molecule itself, Hirshfeld surfaces are defined by the proximity of the molecule itself and its nearest molecular neighbors, as mentioned in Spackman's review [43]. Please refer to [41, 43] for details of concepts, definitions, and what the diagrams represent. Roughly speaking, Hirshfeld surface drawings and the corresponding fingerprint plots serve for visualized insight into intermolecular interactions to form the packing of molecules in crystals. The molecular Hirshfeld surface and 2D fingerprint plots were regarded as quantitative mapping with electrostatic potential, shape-index (delicate changes in shape of surface) and curvedness of the surface (identification of very close intermolecular interactions). The white-colored surface indicates contacts with distances equal to the sum of van der Waals radii, and the red-colored and blue-colored colors mean distances shorter or longer than the van der Waals radii, respectively. The flat areas of the surface stand for the low values of curvedness while the sharp ones indicate the high values of it. The surface drawn as the function of normalized distances di and de, where di (inside atom) and de (outside atom) are the distances from a point on the surface to the nearest atoms.

It is necessary to position the hydrogen atoms precisely and to ensure that the bonding distances to the hydrogen atoms are realistic values. Although hydrogen positions determined using X-ray crystallography may be always biased, Hirshfeld surface analysis is usually used for intermolecular interaction in crystals (not in optimized structures based on DFT calculations). Common treatment of hydrogen atoms involves refinement (geo-metrically calculated positions and riding models), and these can be regarded as statistically reliable hydrogen atom positions in crystals. Furthermore, by considering neutron or electron diffraction, aside from X-ray diffraction, the distance from the Hirshfeld surface to the nearest nucleus within the surface is defined as di; the distance to the nearest nucleus outside the surface is defined as de; and the relationship between di and de for the entire crystal is summarized on a two-dimensional plane, called a two-dimensional fingerprint plot. The plot is colored blue, green, and red as the density of the plot increases on the two-dimensional plane. This plot is known to show a characteristic shape when a particular molecular structure is present and is particularly useful when comparing polymorphic molecules. It is also possible to identify only specific interactions, mapping surfaces where only certain patterns contribute, or display them in a two-dimensional fingerprint plot. The resulting fingerprints show characteristic shapes due to various interactions; typi-

cal examples are indicated by red circles in **Figure 1**. Although it is impossible to refer to the CCDC data, the number of data taken from the CCDC classified into each type of intermolecular interactions are as follows: (a) van der Waals forces (1843 cases); (b) hydrogen bonding (1498 cases); (c) CH-π interactions (789 cases); and (d) π-π interactions (592 cases). This is further discussed in Section 4.

For a long time, our group has synthesized and determined the crystal structures of a variety of novel metal complexes or their organic ligands, such as chiral, polymorphic, and Schiff-base-type molecular crystals. In the next step, particular emphasis has been placed on the hybrid materials of complex molecules binding to proteins. The introduction of artificial metal complexes with organic ligands into proteins is expected to improve their functionality [44]. Indeed, some organometallic complexes (C-coordination) are also possible candidates for metalloprotein designs because they show unique reactivity, which is difficult to obtain using inorganic complexes (e.g., C-C bond formation) [45]. Furthermore, the protein environment provides a variety of different interactions (e.g., hydrogen bonds, hydrophobic and ionic interactions) in the second coordination sphere [46] [47]. Thus, the interaction perspective is considered important for the introduction of guest metal-organic complexes into proteins. The design of metal-organic complexes concerning (surface) hydrophobic pockets of proteins, taking into account their interactions, would lead to an increase in experimental efficiency. One of the tools we can use to visualize intermolecular interactions may be Hirshfeld surface analysis.

This analysis is used not only in metal complexes included by host molecules but also in crystallographically characterized organic ligands, for example. Hirshfeld surface analysis is a theoretical method that yields the visualization of how the whole molecule interacts with its surroundings. This study aims to investigate the relationship between the various features of a molecule and its interactions with other molecules. Although the data obtained are fragmentary, we believe that by investigating specific examples, such as polymorphic molecules

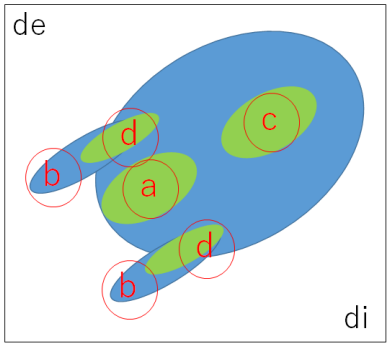

Figure 1. Examples of characteristic shapes of intermolecular interaction in the two-dimensional fingerprints: (a) van der Waals forces; (b) hydrogen bonding; (c) CH-π interactions; and (d) π-π interactions.

with different twist angles and chiral crystallization of achiral molecules, we may be able to deal with various environments in proteins.

2. Methods

Crystal structures (CIF) were obtained from the Cambridge Structure Database (CSD) by CCDC, mainly reported by the authors [48] [49]. Hirshfeld surface analysis was carried out using the CrystalExplorer program [50]. The crystal structure analysis of polymorphic organic molecules [51], crystal-packing achiral molecules in a space group without centrosymmetry [52], organic ligands containing two independent molecules [53], and chiral crystallization due to two types of hydrogen bonds [54] was conducted to discuss the molecular shape and crystal packing of these molecules. We performed Hirshfeld surface analysis on crystallographically characterized molecules. In the next section, we review the results of Hirshfeld surface analysis of not only metal complexes, but also organic compounds (as ligands), mainly reported in our laboratory so far.

3. Review of Hirshfeld Surface Analysis of the Crystals

Hirshfeld surface analyses were newly performed on the crystalline compounds published by our laboratory so far. Molecules with some characteristic structures were picked up and reviewed. In this section, we discuss molecular features and intermolecular interactions of the crystals, comparing conventional methods (observation of crystal structures) and Hirshfeld surface analysis. However, primarily due to space considerations, the fingerprints only include a select few of the major interactions. In principle, this analysis can output quantitative values for all types, but if there is a difference compared to judgment by conventional observation, its accuracy, and characteristics (and bias, if any, depending on the judgment method) should be considered) can be read. For example, there are some cases where Hirshfeld surface analysis does not show a bond involving a halogen because the contribution rate is low.

3.1. (Z)-1-Benzoyl-5-benzylidene-2-hydroxy-4-oxo-4,5-di-hydro-1H-pyrrole-3-carbonitrile

An example of the crystallization of achiral molecules in a space group without cetrosymmetry is described in [55]. This is the first crystal structure reported for chiral crystallization of a pyrrole of this type. Conventional investigation suggests that O-H···N hydrogen bonds link the molecules, which may potentially contribute to this characteristic "chiral crystallization", while intramolecular O-H···O bonds also occur in the crystal. Hirshfeld surface analysis suggests that molecular bonds are strong due to H···H interactions. Other O···H interactions are thought to act mainly on the sides of the molecules (**Figure 2**). The red-colored area of the surface is consistent to the hydrogen bonding features. The fingerprint for all interactions indicates characteristics of (a) van der Waals forces, (b) hydrogen bonding and (c) CH-π interactions.

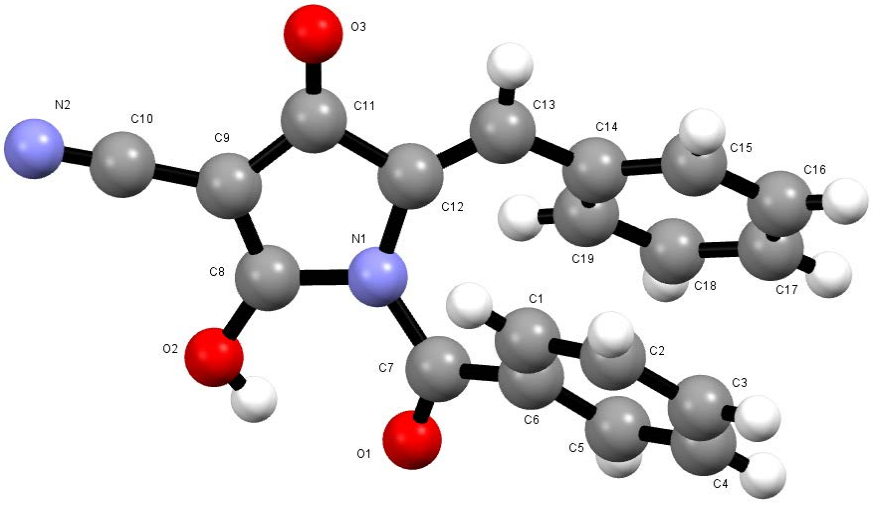

(a)

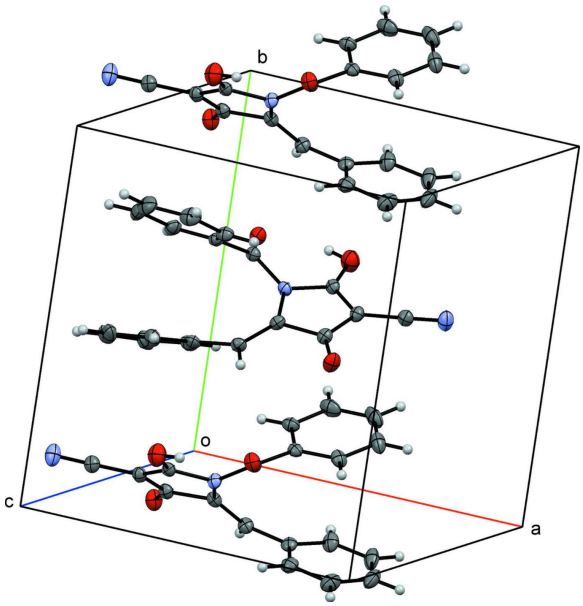

(b)

Figure 2. (a) Molecule and (b) packing of this crystal.

3.2. 4,4'-(1,2-Diazaniumylethane-1,2-diyl) Dibenzoate Trihydrate

Themolecule of title compound crystallizes as a zwitterion with protonated amine groups NH_3^+ and deprotonated carboxylate groups COO^- is presented in [56]. In addition to electrostatic interactions between positively and negatively charged moieties, in this crystal, N-H···O and O-H···O hydrogen bonds link (totally neutral) molecules into a three-dimensional network. O···H interactions are particularly pronounced, suggesting that the molecules are strongly linked to each other via crystalline water molecules (**Figure 3**). The extended π-conjugated systems from phenyl groups may also enhance π interaction involving hydrogen atoms, as shown by Hirshfeld surface analysis. In addition, there also are two asymmetric carbon atoms (both are R configuration) in the title compound,

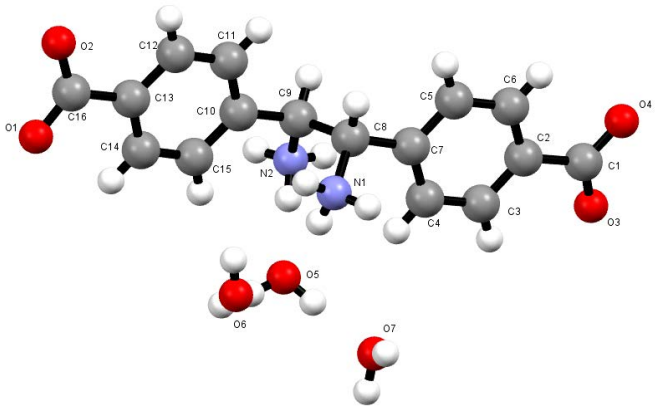

Figure 3. Molecule and of this crystal.

resulting in a chiral space group. The red-colored area of the surface is consistent to the hydrogen bonding features. The fingerprint for all interactions indicates characteristics of (a) van der Waals forces and (b) hydrogen bonding interactions.

3.3. 4-Phenyldiazenyl-2-[(R)-(1-phenylethyl) iminomethyl] Phenol

A chiral photochromic Schiff-base compound is described in [57]. An intramolecular O-H···N hydrogen bond can only be formed when phenol-imine tautomers take an appropriate form. C···H interactions are prominent, and the molecules are thought to be linked together by aligning parallel to the benzene ring (**Figure 4**). There are three phenyl rings in these molecules. The azobenzene moiety, composed of two of the three, adopts a trans form against N=N bonds. In contrast to Hirshfeld surface analysis, however, the original paper did not point out characteristic intermolecular interactions based on conventional observations. The small red-colored area of the surface is consistent to the lack of intermolecular hydrogen bonding features. The fingerprint for all interactions indicates characteristics of (c) CH-π interactions mainly.

3.4. 6-[(R)-(2-Hydroxy-1-phenylethyl) aminomethylidene]-4-(2-phenyl-diazen-1-yl) cyclohexa-2,4-dien-1-one

A further chiral photochromic Schiff-base compound containing azobenzene moiety is described in [58]. This molecule exhibits a keto-amine tautomeric form (potentially acting as intramolecular hydrogen sites) and displays characteristic features of azobenzene derivatives of trans (E) conformation. The hydroxy group is also involved in an intermolecular hydrogen bond between O-H···O sites. C···H interactions are prominent, suggesting H interaction with the benzene ring due to the twisting of the molecule. The diazenyl group is involved in π interactions, which is supported by Hirshfeld surface analysis, too. Because of the hydroxyl group, partially strong O···H interactions can also be observed (**Figure 5**). The red-colored area of the surface is consistent to the hydrogen

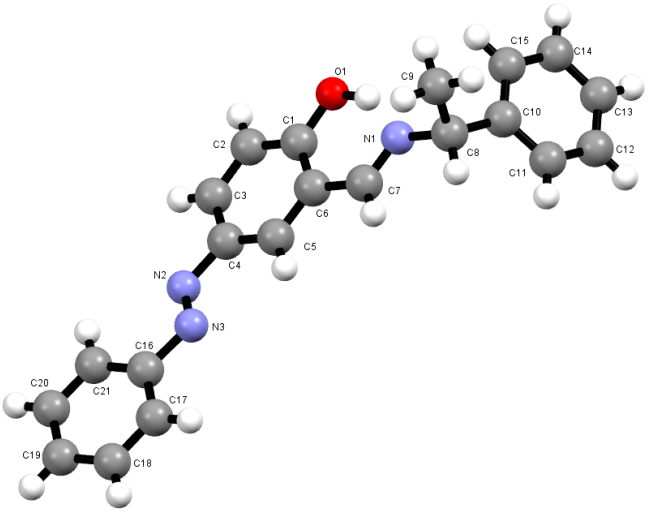

Figure 4. Molecule and of this crystal.

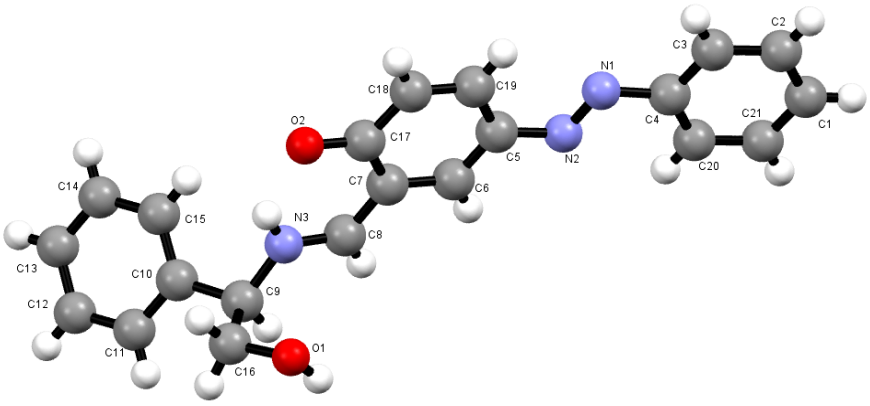

Figure 5. Molecule of this crystal.

bonding features. The fingerprint for all interactions indicates characteristics of (b) hydrogen bonding predominantly.

3.5. (R)-4-bromo-2-[(1-phenylethyl) iminomethyl] Phenol

A chiral Schiff base compound possessing photochromic properties due to imine and phenol groups is described in [59]. The molecule is a phenol-imine tautomer, and there is an intramolecular O-H···N hydrogen bond. The planarity of this molecule, with two six-membered phenyl rings, is also stabilized by an intra-molecular O-H···N hydrogen bond. H···H interactions are prominent, but the proportion of C···H interactions is also high, suggesting that the folded structure of the molecule affects the interactions of the Br group (**Figure 6**). Contrary to Hirshfeld surface analysis, however, halogen involving hydrogen bonds was not mentioned in the original paper based on conventional observations. The small red-colored area of the surface is consistent to the lack of intermolecular hydrogen bonding features (almost not acting halogen atoms). The fingerprint for all interactions indicates characteristics of (c) CH-π interactions.

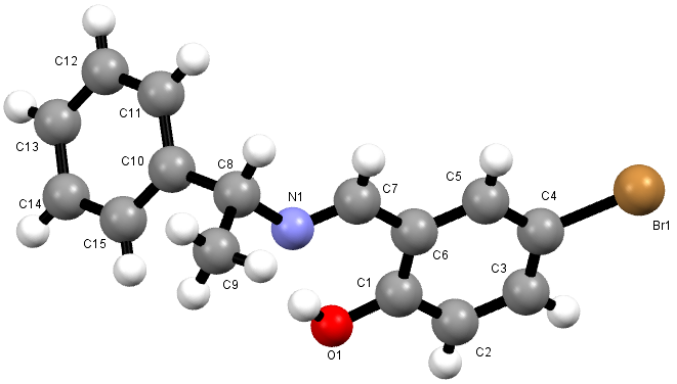

Figure 6. Molecule of this crystal.

3.6. (R)-4-methoxy-2-[(1-phenylethyl) iminomethyl] Phenol

A chiral (also potentially photochromic) Schiff base compound is described in [60]. The title compound potentially adopted the phenol-imine tautomeric form, which may be involved in intramolecular O-H···N hydrogen bonds when suitably formed. H···H interactions are prominent, but the proportion of C···H interactions is also high, suggesting that the folded structure of the molecule affects weak interactions via the methoxide group (**Figure 7**). Crystal packing is also stabilized by two C-H···π interactions involving the aromatic ring with a considerable dihedral angle between them. The small red-colored area of the surface is consistent to the lack of intermolecular hydrogen bonding features. The fingerprint for all interactions indicates characteristics of (a) van der Waals forces, (c) CH-π interactions and (d) π-π interactions.

3.7. bis(N-methylethylenediamine-*κ*2N, N') bis(perchlorate-*κ*O) copper(II)

Thetitle compound is neutrally charged as a crystal, although it is composed of cation (copper(II) complex) and anion (perchlorate) moieties. Although electrostatic interactions may be expected, N-H···O hydrogen bonds were predominantly reported in the original paper based on conventional observation. This main part is a cation of a copper(II) complex with ethylene diamine ligands showing Jahn-Teller distortion [61], which may be weaker than normal covalent bonds in a crystal. According to Hirshfeld surface analysis, H···H interactions and O···H interactions are prominent, with partially strong interactions observed in the O···H interactions via perchlorate anions (**Figure 8**). The red-colored area of the surface is consistent to the hydrogen bonding features as well as electrostatic interactions. The fingerprint for all interactions indicates characteristics of (a) van der Waals forces and (b) hydrogen bonding.

3.8. Bis (5-chloro-N-iso-propyl-salicyldenaminato-*κ*2N, O) copper(II)

This title compound is a neutral coordination compound involving Schiff base ligands adopts a stepped conformation and affords square-planar trans-[CuN_2O_2]

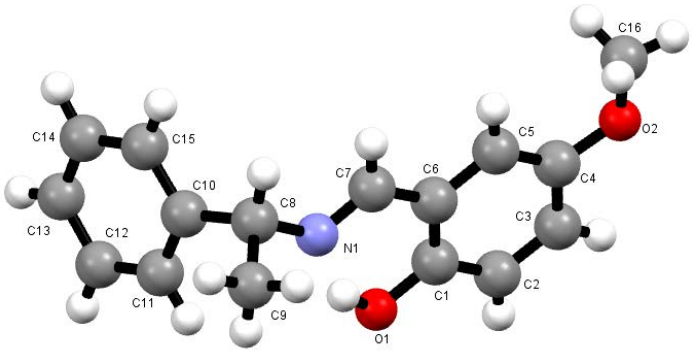

Figure 7. Molecule of this crystal.

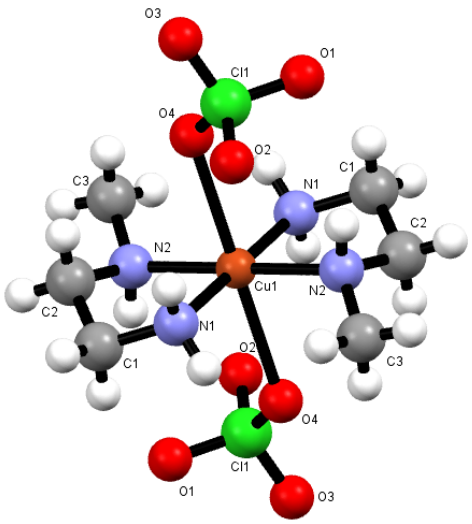

Figure 8. Molecule of this crystal.

coordination geometry, in which the Cu(II) ion lies on the center of symmetry [62]. Crystal packing may be flexible because the related compounds occur during phase transition according to temperature changes. Indeed, the original paper stated that crystal packing was predominantly controlled by weak van der Waals forces. No particularly strong interactions were observed, as stated in the original paper based on conventional observation, and this is thought to be constituted by weak linkages due to H···H interactions, regardless of Cl group (**Figure 9**). Halogen atoms may be expected to contribute to intermolecular interactions based on Hirshfeld surface analysis. The small red-colored area of the surface is consistent to the lack of intermolecular hydrogen bonding features (almost not acting halogen bonding). The fingerprint for all interactions indicates characteristics of (a) van der Waals forces and (c) CH-π interactions.

3.9. Bis (N-ethylethylenedi-amine-κ2N, N') copper(II)-hexacyanocobaltate(III)-water (3/2/4): A Two-Dimensional Ladder Structure of a Bimetallic Assembly

This title compound is a two-dimensional coordination polymer is structurally

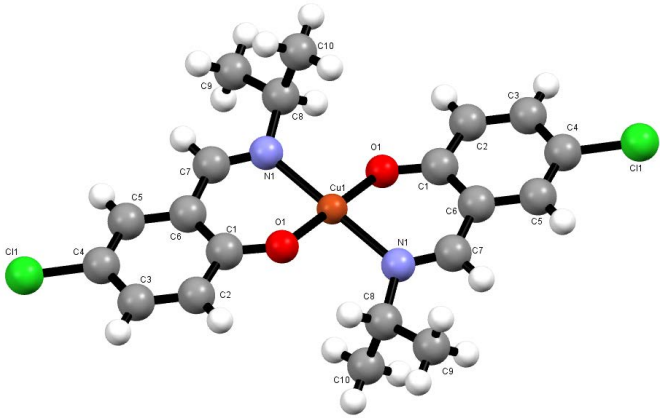

Figure 9. Molecule of this crystal.

characterized by new two-dimensional cyano-bridged Cu(II)-Co(III) bimetallic assembly [63]. This neutral compound is composed of both the cations of the Cu(II) complex and the anion of the Co(III) complex. However, in the original paper based on conventional observation, (ligand of Cu(II) moiety) N-H···H (ligand of Co(III) moiety) interactions were mentioned in the two-dimensional networks of coordination bonds. This feature could be deeply considered using Hirshfeld surface analysis. Between the two-dimensional structures, H···H interactions can be prominently identified (**Figure 10**). The red-colored area of the surface is consistent to the hydrogen bonding features involving water molecules crystalline solvent besides electrostatic interaction. The fingerprint for all interactions indicates characteristics of (b) hydrogen bonding apparently.

3.10. (E)-3-[(2,6-dimethylphenyl) diazenyl]-7-methyl-1H-indazole

The title compound is a neutral organic compound with azo-(-N=N-) bond moiety and a pyrazole moiety [64]. In the crystal of the title compound, helically zigzag chains along the b-axis direction with C(3) as a graph-set motif are formed by N-H···N intermolecular hydrogen bonds of pyrazole moieties. Moreover, two types of C-H···π interactions were also pointed out in the original paper based on conventional observations. This intermolecular interaction resulted in chiral crystallization. According to Hirshfeld surface analysis, the main interaction is H···H, and C···H interactions can be identified in the two benzene rings. Partially strong N···H interactions are also observed (**Figure 11**). The red-colored area of the surface is consistent to the hydrogen bonding features. The fingerprint for all interactions indicates characteristics of (b) hydrogen bonding mainly.

3.11. 2-{(R)-[1-(4-bromophenyl) ethyl] iminomethyl}-4-(phenyldiazenyl)phenol

The title compound is a chiral (asymmetric carbon) photochromic (both azobenzene moiety and imine and phenol groups) Schiff-base compound that is

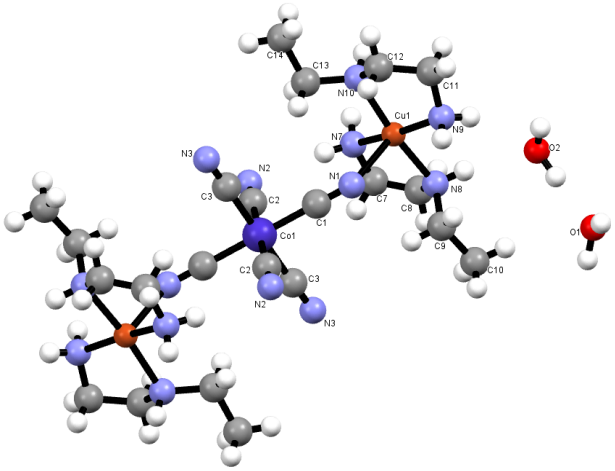

Figure 10. Molecule of this crystal.

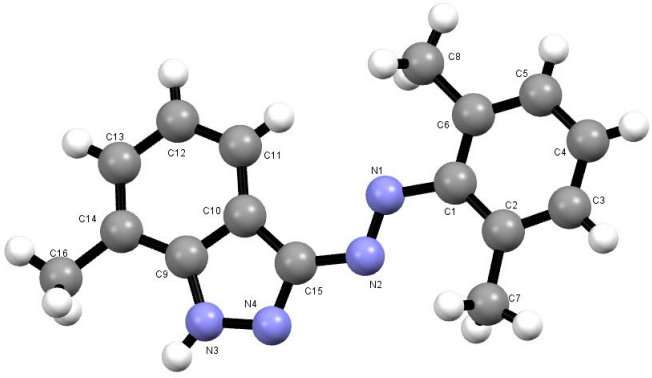

Figure 11. Molecule of this crystal.

neutrally charged [65]. The molecule determined that its crystal structure corresponds to the phenol-imine tautomer. As the original paper stated, the hydroxy group is involved in intramolecular O-H···N hydrogen bonding. In addition, three types of C-H···π interactions supported crystal packing, forming one-dimensional chains that were detectable by conventional observation. Only Hirshfeld surface analysis suggested short intermolecular Br···H contacts besides them. Nevertheless, in the Br group with halogen bonding potential, H···H interactions are prominent, but C···H interactions can also be identified in the benzene ring (**Figure 12**). The small red-colored area of the surface is consistent to the lack of intermolecular hydrogen bonding features. The fingerprint for all interactions indicates characteristics of (c) CH-π interactions (not acting halogen bonds).

3.12. 3,6-dihydroxy-4,5-dimethylbenzene-1,2-dicarbaldehyde

This is an achiral, neutral, and almost simple planar compound that interestingly crystallizes in a space group without centrosymmetry (sometimes called "chiral crystallization") [66]. Between these planar molecules, some localized O···H interactions (five types were pointed out in the original paper) can be identified by

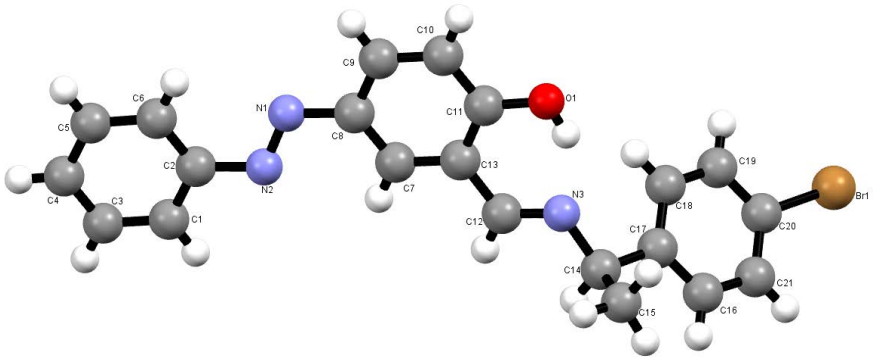

Figure 12. Molecule of this crystal.

Hirshfeld surface analysis, and loose C···H interactions of C-H···π type are also seen to form helical crystal packing with two-fold axis to form $P2_1$. (**Figure 13**). However, according to a database survey in the original paper, not all analogous compounds with C-H···O interactions were crystallized in non-centrosymmetry space groups. The red-colored area of the surface is consistent to the hydrogen bonding features. The fingerprint for all interactions indicates characteristics of (b) hydrogen bonding and (c) CH-π interactions.

3.13. Bis[cis-(1,4,8,11-tetraazacyclotetradecane-*κ*4N) bis(thiocyanato-*κ*N) chromium(III)] di-chromate Monohydrate

The asymmetric unit comprises one $[Cr(NCS)_2(cyclam)]^{2+}$ cation, half of a $Cr_2O_7^{2-}$ anion (completed by inversion symmetry), and half of a water molecule [67]. Regarding the composition, this crystal may be expected to be straightforwardly dominated by electrostatic inter-actions. The original paper explained the packing formation feature as follows: "The crystal is stabilized by intermolecular hydrogen bonds of the cyclam N-H groups and water O-H groups (donors) and the O atoms of $Cr_2O_7^{2-}$ or water molecules (acceptor) to form a three-dimensional network." Local O···H interactions can also be identified by conventional observations (**Figure 14**). In addition to H···H interactions, S···H interactions can be identified only by Hirshfeld surface analysis. The small red-colored area of the surface is consistent to the predominant electrostatic interactions between cations and an-ions. The fingerprint for all interactions indicates characteristics of (b) hydrogen bonding.

3.14. Hexakis-(urea-*κ*O) chromium(III) Dichromate Bromide Monohydrate

This crystal is also composed of a cation of the Cr(III) complex and an anion of the $Cr_2O_7^{2-}$ unit, which could be expected to have predominant electrostatic interactions [68]. Within the complex cation, the Cr(III) atom is coordinated by six O atoms of six urea ligands, dis-playing a slightly distorted octahedral coordination environment. There is also Br^- (ready for electrostatic interaction) in

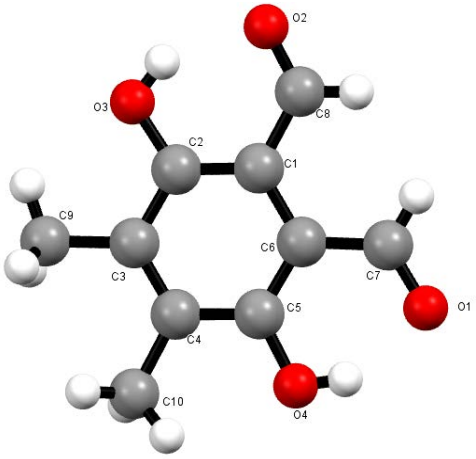

Figure 13. Molecule of this crystal.

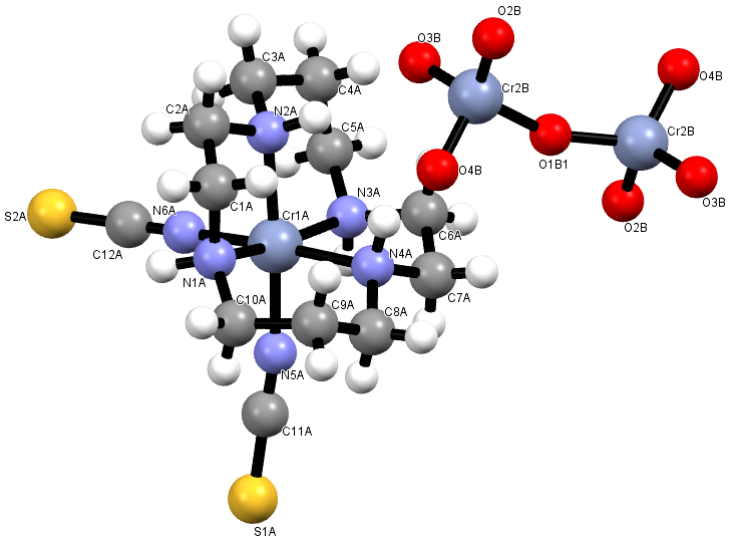

Figure 14. Molecule of this crystal.

the crystal as a counter anion. Local O···H interactions can be seen even by conventional observations, which accounts for a large proportion of the total interaction (**Figure 15**). Aside from electrostatic force, Br^- links the Cr(III) complex and water molecules via N-H···Br and O-H···Br hydrogen bonds. The supramolecular architecture of a three-dimensional network also includes N-H···O and O-H···O hydrogen bonds between urea N-H and water O-H donor groups, as well as O atoms of the $Cr_2O_7^{2-}$ anions. Thus, there are several types of hydrogen bonds, even in the ionic crystals of anions and cations. The red-colored area of the surface is consistent to the hydrogen bonding features. The fingerprint for all interactions indicates characteristics of (a) van der Waals forces and (b) hydrogen bonding (halogen atoms as hydrogen acceptors were not clear).

3.15. 3,5-dichloro-2-{[(1-phenylethyl) imino] methyl} Phenol

The title compound is a chiral (associated with asymmetric carbon) Schiff base

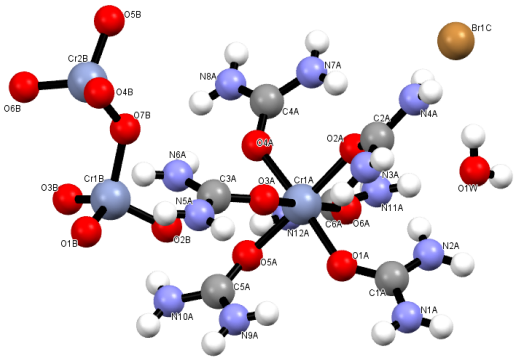

Figure 15. Molecule of this crystal.

compound that synthesized from racemic 1-phenylethylamine and 3,5-dichlorosalicyl-aldehyde [69]. Aside from molecular recognition of racemic pairs of molecules, there is no possibility of structural control of chirality (at least in terms of asymmetric arrangement of molecules). The π-conjugate system around the imine group is essentially planar in the phenol-imine tautomer. The latter is prepared for intramolecular O···N hydrogen bonds. Intermolecular C-H···π interactions are also present in the crystal structure. Moreover, Cl···H interactions are detectable. According to a close investigation using Hirshfeld surface analysis, this is attributed to the folded structure of the molecule, which makes it easier for the H bonded to the C15 atom to approach the Cl atom (**Figure 16**). The small red-colored area of the surface is consistent to the lack of intermolecular hydrogen bonding features. The fingerprint for all interactions does not indicate characteristics of (a) van der Waals forces, (b) hydrogen bonding, (c) CH-π interactions nor (d) π-π interactions but Cl···H interactions.

3.16. 1-(2-iodo-benzo-yl)-4-(pyrimidin-2-yl) Piperazine

In this title neutral compound, which involves the I atom, the central six-membered piperazine ring adopts an almost perfect chair conformation with the pyrimidine substituent in an equatorial site [70]. The original paper stated that C-H···O and C-H···π(arene) hydrogen bonds made the molecules form a three-dimensional network structure and presented the augmentation by π-π stacking interactions and an I···N halogen bond. These facts could be detected by conventional observations of the crystal structures. A high proportion of H-H interactions, as well as local O-H interactions involving the C=O group, can be identified, regardless of potentially polar I group (**Figure 17**). These features could be discussed following Hirshfeld surface analysis 18. The small red-colored area of the surface is consistent to the lack of intermolecular hydrogen bonding features. The fingerprint for all interactions indicates characteristics of (a) van der Waals forces and (b) hydrogen bonding.

3.17. trans-Bis(2,2-diphenylethylamine-κN) bis(5,5-diphenylhydantoinato-κN3) copper(II)

Guest molecules of solvents may sometimes induce structural changes in the

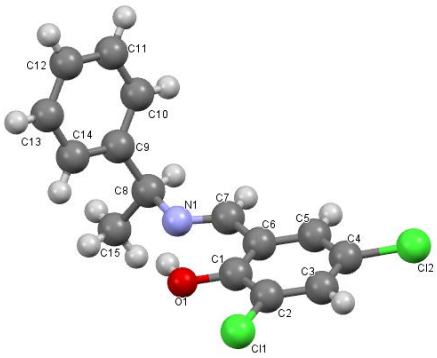

Figure 16. Molecule of this crystal.

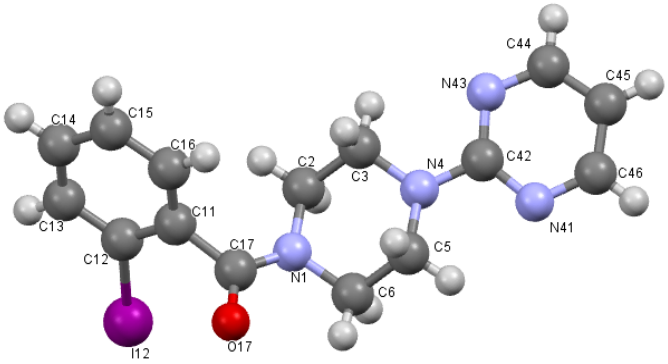

Figure 17. Molecule of this crystal.

host molecules of crystals. The title neutral complex affords a distorted square-planar [CuN_4] coordination environment (blue-violet colored), in which the Cu(II) atom lies on the center of symmetry when containing a chloroform solvent [71]. While a square-planar [CuN_4] complex (reddish-violet colored) could be obtained for the solvent free crystal. Using am-ide moiety of hydantoin rings, double complementary N-H···O intermolecular hydrogen bonds could be formed in both cases, which may play an important role in forming crystal packing. According to Hirshfeld surface analysis of the solvent-containing crystal, H···H interactions are prominent, but C···H interactions can also be identified (**Figure 18**), which could not be found via conventional observations. The red-colored area of the surface is consistent to the hydrogen bonding features. The fingerprint for all interactions indicates characteristics of (a) van der Waals forces and (b) hydrogen bonding. The chloroform molecule does not contribute significantly to intermolecular hydrogen bonding. Rather, it acts as a blocker for normal hydrogen bonding packing.

3.18. trans-Bis(5,5-diphenylhydantoinato) bis(2-phenylethylamine) copper(II)

A similar example to the previous one is introduced here. This crystal structure is also mainly stabilized by two anti-parallel N-H···O=C intermolecular hydrogen bonds. This compound affords a square-planar trans-[CuN_4] coordination environment, while the Cu(II) atom lies on a center of symmetry. Both 5,5-diph-

enyl-hydantoinate and 2-phenylethylamine ligands behave as monodetate ligands and bind to the central Cu(II) ion through their N atoms [72]. A high proportion of H···H interactions and local O···H interactions can be identified using Hirshfeld surface analysis, though hydantoin rings have amide moieties ready for hydrogen bonds toward neighboring molecules (**Figure 19**). This feature also supports the role of solvent molecules in the previous example. The red-colored area of the surface is consistent to the hydrogen bonding features. The finger-print for all interactions indicates characteristics of (a) van der Waals forces and (b) hydrogen bonding. It can be regarded as the case where there is no factor inhibiting packing by ordinary hydrogen bonding.

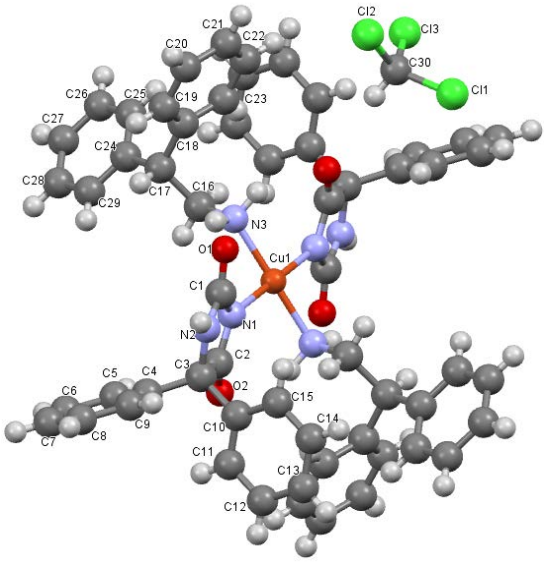

Figure 18. Molecule of this crystal.

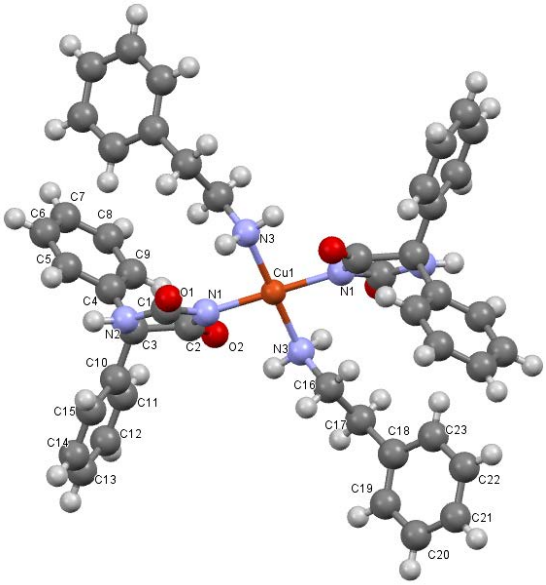

Figure 19. Molecule of this crystal.

4. Statistical Investigation of Hirshfeld Surface Analysis as Datasets

Focusing on the versatility and quantification of the Hirshfeld surface analysis, we draw a large amount of data from databases other than the crystal structures we reported, and consider the limits that can (or cannot) be discussed. Therefore, the following statistical investigation was attempted. As far as we know, at least in the crystal structures of "organic", "small molecule" and "single crystal" X-ray crystallography, there are almost no research examples that have obtained certain knowledge by machine learning from Hirshfeld surface analysis and fingerprint big data. Therefore, here we propose a point of view that can be discussed from the usual statistical correlation.

While the analysis of individual CIF data has been used to investigate the intermolecular interactions of crystallographically characteristic molecules, it is also possible to carry out statistical investigations by analyzing a large number of data and subsequently extracting information. This is based on the hypothesis that the results from Hirshfeld surface analysis are data that contain all the information written on the CIF, such as the position and type of atoms, bond lengths, electrostatic potentials, etc. This can then be output them in terms of molecular interactions. The method used in this statistical investigation is a type of unsupervised learning called principal component analysis. In this method, various interactions are evaluated and aggregated, and the two components with the highest contribution rate are set as the main components and plotted on a graph on a two-dimensional plane with two main components as the axes to investigate correlations [73]. In the present study, Hirshfeld analysis was performed on approximately 1000 CIF data to determine the proportion of H···H, C···H, C···C, and O···H interactions in the overall interaction of the molecule. The C···H interaction includes the cases of H inside the Hirshfeld surface and C outside the surface, while the O···H interaction includes the cases of H inside the surface and O outside the surface. By performing unsupervised learning on the data collected in this way, it is possible to find some correlation between the molecular features and the type and proportion of interactions. A survey of the complexes obtained in our laboratory showed that the more crystalline water molecules there were, the higher the contribution of hydrogen bonding tended to be. Therefore, we decided to investigate the correlation between the number of crystalline water molecules and the contribution of intermolecular interactions and performed Hirshfeld surface analysis on about 1000 CIF files collected from the CCDC to determine the contribution of four types of intermolecular interactions (**Figure 20**).

As for statistical analysis, quantitative treatment may be beyond reliable examination. The number of water with different situations of hydrogen bonds should not be discussed as valuables of function but merely (chemically rational) appearance characteristics of the scatter plot. As can be seen from the figure, the further crystalline water molecules increase, the further O···H interaction

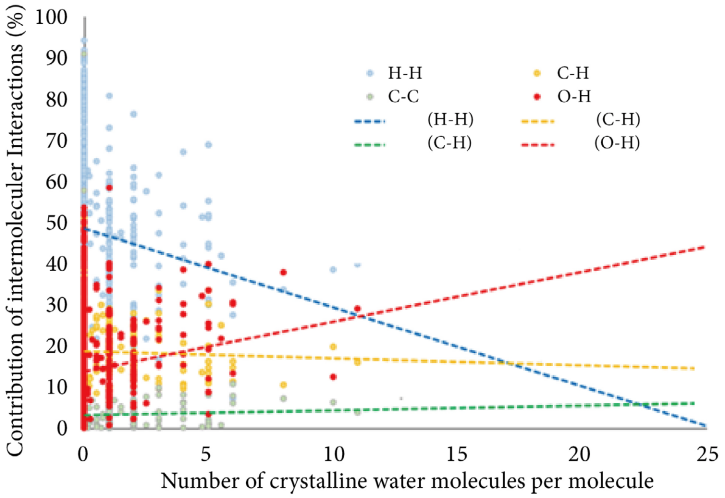

Figure 20. Statistical plots of the contribution of intermolecular interactions *vs.* a number of crystalline water molecules per molecule for crystal structures investigated using Hirshfeld surface analysis in this study. Colors denote four types of intermolecular interactions. Dashed lines denote qualitative tendency.

increases and the further H···H interactions decrease. In addition, the contribution of the C···C interaction and the C···H interaction did not change. This indicates that these two interactions are not affected by the number of crystalline water molecules. This result indicates that the presence of water molecules strengthens bonding via intermolecular interactions in a certain direction. Furthermore, crystalline water contributes little to the benzene ring and is selectively arranged.

5. Conclusions and Perspective

In summary, one of the notable advantages of the Hirshfeld surface analysis is the interaction between hydrogen atoms based on subtle differences in electronegativity, which tends to be neglected by conventional visual confirmation. Along the recent examples mentioned in introduction (Section 1), brief classification of the results for our crystal structures in Section 3 is as follows:

- Aggregation due to van der Waals interaction (too weak interaction to detect): 3.4, 3.8 (almost no contribution from halogen atoms);
- CH-π interactions: 3.5 (almost no contribution of halogens), 3.6, 3.12 (halogens also participate), 3.13 ordinary hydrogen bonding and CH-π (chiral crystallization of planar 6-membered ring neutral molecules);
- π-π interaction: 3.17 (halogen hydrogen bond is weak);
- Ordinary hydrogen bonds: 3.1, 3.19 (two between neutral molecules, no chloroform solvent);
- Weak hydrogen bonds: 3.11, 3.18 (weakened by chloroform solvent);
- Halogen hydrogen bond: 3.16 (where the role of Cl is clear);
- Heteroatom hydrogen bond: 3.14 (when S is involved in ionic crystals);
- Both hydrogen bonding and electrostatic attraction; 3.4 (protonated organic

molecules);

- Covalently interactions between same type atoms: Quantitatively, H···H interactions are often dominant, but can also be attributed to other classifications. There were no examples of interactions between halogens and metals;
- Ionic crystals of metal complexes: 3.7, 3.10 (hydrogen bonds with water of crystallization), 3.15 (both electrostatic bonds and ordinary hydrogen bonds).

In the previous section, we introduced seemingly random cases, but it is rather convenient to summarize trends without preconceptions. The intermolecular interactions described above are arranged in order of what is usually considered to be the weakest to the strongest. The strong ones should make an important contribution to maintaining crystal packing, while the weak ones should make an essential contribution to molecular recognition together with the shape of the substituents. Here, the two-dimensional fingerprints are limited to those with quantitatively large numerical values.

Quantitative analysis was carried out using Hirshfeld surface analysis to study molecular interactions. Using this method, it is possible to determine not only which parts of a molecule contribute to an interaction, but also the proportion of that interaction in the total molecular interaction. It is also possible to determine the contribution of not only visually obvious interactions, such as the O···H interaction and the C···C interaction, but also the contribution of interactions that are difficult to notice, such as the C···H interaction and the N···H interaction, H interactions and N···H interactions. In particular, as complexes often have a spherical molecular shape, the contribution of C···H interactions to the overall molecular interaction ratio is considered to be higher in many cases than that of local O···H interactions. In addition, as intermolecular interactions in crystals were investigated in the present study, it is considered that the molecules are rarely flattened and the contribution of C···C interactions is low in many cases, considering that the complexes are spherical in shape. Even in the example of chiral crystallization of the complex, the contribution of C···H interactions to the contribution of the helical arrangement is high, and even in the example of polymorphic molecules, the contribution of C···H interactions is higher for molecules with a twisted shape than for molecules with a flat shape. The need to consider C···H interactions may increase as molecules become bulkier in molecular de-sign. The contribution of O···H interactions may also be higher in the case of crystals forming a network through water molecules. The O···H interactions in this case is likely to be localized at the Hirshfeld surface and is often strong interactions that anchor molecules. This perspective of interactions has the potential to influence the molecular design of metal complexes, such as ligands, for complexation with proteins.

In our laboratory, for example, there is also a copper(II) complex reported by us [74], binding to egg white lysozyme. The functional groups of the protein have been observed to coordinate or interact with sites on the Hirshfeld surface of the complex that are marked as strongly interacting (**Figure 21**). Thus, the

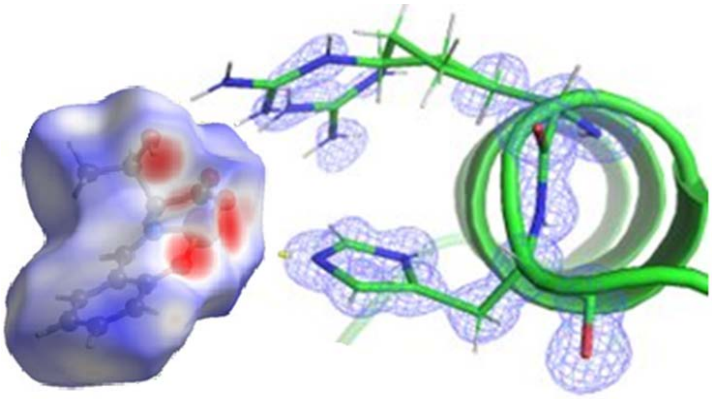

Figure 21. Proposed structure of docking of protein residues and small molecule (indicating Hirshfeld surface) *via* hydrogen bonds.

appearance of intermolecular interactions in crystals may be used to examine interactions in solvents. Actually, we have obtained crystal structure of egg white lysozyme binding by a metal complex [75]. Without chemical bonds (only intermolecular interactions), however, it may be quite difficult to obtain single crystals of proteins including metal complexes at least experimentally [76]. Considering complexation with proteins, it is necessary to examine not only intermolecular interactions, but also coordination bonds using Hirshfeld surface analysis in the near future.

Acknowledgements

This work was partly supported by a Grant-in-Aid for Scientific Research (A) KAKENHI (20H00336).

Conflicts of Interest

The authors declare no conflicts of interest regarding the publication of this paper.

References

[1] Gellman, S.H. (1997) Introduction: Molecular Recognition. *Chemical Reviews*, **97**, 1231-1232. https://doi.org/10.1021/cr970328j

[2] Zeng, W., Wang, X., Zhou, T. and Zhang, Y. (2023) Crystal Structure, Photophysical Study, Hirshfeld Surface Analysis, and Nonlinear Optical Properties of a New Hydroxyphenylamino Meldrum's Acid Derivative. *Molecules*, **28**, Article No. 2181. https://doi.org/10.3390/molecules28052181

[3] Kumar, M., Jaiswar, G., Afzal, M., Muddassir, M., Alarifi, A., Fatima, A., Siddiqui, N., Ayub, R., Abduh, N.A.Y., Saeed, W.S. and Javed, S. (2023) Quantum Computational, Spectroscopic (FT-IR, FT-Raman, NMR, and UV-Vis) Hirshfeld Surface and Molecular Docking-Dynamics Studies on 5-Hydroxymethyluracil (Monomer and Trimer). *Molecules*, **28**, Article No. 2116. https://doi.org/10.3390/molecules28052116

[4] Semenova, L.I., Ling, I. and Sobolev, A.N. (2023) Chirality as a Feature of the Crystal Structure of Lanthanide Ion Complexes—Some Simple Examples. *Crystals*, **13**,

Article No. 337. https://doi.org/10.3390/cryst13020337

[5] Bojarska, J., Breza, M., Remko, M., Czyz, M., Gajos-Michniewicz, A., Zimecki, M., Kaczmarek, K., Madura, I.D., Wojciechowski, J.M. and Wolf, W.M. (2022) Structural and Biofunctional Insights into the Cyclo(Pro-Pro-Phe-Phe-) Scaffold from Experimental and *in Silico* Studies: Melanoma and Beyond. *International Journal of Molecular Sciences*, **23**, Article No. 7173. https://doi.org/10.3390/ijms23137173

[6] Craciun, N., Chisca, D., Melnic, E. and Fonari, M.S. (2023) Unprecedented Coordination Compounds with 4,4'-Diaminodiphenylethane as a Supramolecular Agent and Ditopic Ligand: Synthesis, Crystal Structures and Hirshfeld Surface Analysis. *Crystals*, **13**, Article No. 289. https://doi.org/10.3390/cryst13020289

[7] Deeloed, W., Wannapaiboon, S., Pansiri, P., Kumpeerakij, P., Phomphrai, K., Laobuthee, A., Hanlumyuang, Y., Suramitr, S., Pinyou, P. and Wattanathana, W. (2020) Crystal Structure and Hirshfeld Surface Analysis of Bis(Triethanolamine)Nickel(II) Dinitrate Complex and a Revelation of Its Characteristics via Spectroscopic, Electrochemical and DFT Studies towards a Promising Precursor for Metal Oxides Synthesis. *Crystals*, **10**, Article No. 474. https://doi.org/10.3390/cryst10060474

[8] Gacki, M., Kafarska, K., Pietrzak, A., Korona-Głowniak, I. and Wolf, W.M. (2020) Quasi-Isostructural Co(II) and Ni(II) Complexes with Mefenamato Ligand: Synthesis, Characterization, and Biological Activity. *Molecules*, **25**, Article No. 3099. https://doi.org/10.3390/molecules25133099

[9] Krupka, K.M., Banach, S., Pocheć, M., Panek, J.J. and Jezierska, A. (2023) Making and Breaking—Insight into the Symmetry of Salen Analogues. *Symmetry*, **15**, Article No. 424. https://doi.org/10.3390/sym15020424

[10] Mahmoudi, G., Kumar Seth, S., Bauza Riera, A., Ivanovich Zubkov, F. and Frontera, A. (2020) Novel Pb(II) Complexes: X-Ray Structures, Hirshfeld Surface Analysis and DFT Calculations. *Crystals*, **10**, Article No. 568. https://doi.org/10.3390/cryst10070568

[11] Noor, A. (2022) Crystallographic Evidence of η1-Coordination of Bulky Aminopyridine in Halide-Containing Iron(II) Complexes. *Crystals*, **12**, Article No. 697. https://doi.org/10.3390/cryst12050697

[12] Masternak, J., Zienkiewicz-Machnik, M., Łakomska, I., Hodorowicz, M., Kazimierczuk, K., Nosek, M., Majkowska-Młynarczyk, A., Wietrzyk, J. and Barszcz, B. (2021) Synthesis and Structure of Novel Copper(II) Complexes with N,O- or N,N-Donors as Radical Scavengers and a Functional Model of the Active Sites in Metalloenzymes. *International Journal of Molecular Sciences*, **22**, Article No. 7286. https://doi.org/10.3390/ijms22147286

[13] Altowyan, M.S., Haukka, M., Soliman, S.M., Barakat, A., Alaswad, S.O., Boraei, A.T.A., Gad, E.M. and Youssef, M.F. (2023) Synthesis, Characterization and Single Crystal X-Ray Diffraction Analysis of Fused Triazolo/Thiadiazole Clubbed with Indole Scaffold. *Crystals*, **13**, Article No. 423. https://doi.org/10.3390/cryst13030423

[14] Ghazzy, A., Taher, D., Korb, M., Al Khalyfeh, K., Helal, W., Amarne, H., Rüffer, T., Ishtaiwi, Z. and Lang, H. (2022) Rearrangement of Diferrocenyl 3,4-Thiophene Dicarboxylate. *Inorganics*, **10**, Article No. 96. https://doi.org/10.3390/inorganics10070096

[15] Altowyan, M.S., Khalil, S.M.S.M., Al-Wahaib, D., Barakat, A., Soliman, S.M., Ali, A.E. and Elbadawy, H.A. (2022) Synthesis of a Novel Unexpected Cu(II)-Thiazolidine Complex—X-Ray Structure, Hirshfeld Surface Analysis, and Biological Studies. *Molecules*, **27**, Article No. 4583. https://doi.org/10.3390/molecules27144583

[16] Seth, S.K. (2018) The Importance of CH···X (X=O, π) Interaction of a New Mixed

Ligand Cu(II) Coordination Polymer: Structure, Hirshfeld Surface and Theoretical Studies. *Crystals*, **8**, Article No. 455. https://doi.org/10.3390/cryst8120455

[17] Baykov, S.V., Mikherdov, A.S., Novikov, A.S., Geyl, K.K., Tarasenko, M.V., Gureev, M.A. and Boyarskiy, V.P. (2021) π-π Noncovalent Interaction Involving 1,2,4- and 1,3,4-Oxadiazole Systems: The Combined Experimental, Theoretical, and Database Study. *Molecules*, **26**, Article No. 5672. https://doi.org/10.3390/molecules26185672

[18] Jmai, M., Gatfaoui, S., Issaoui, N., Roisnel, T., Kazachenko, A.S., Al-Dossary, O., Marouani, H. and Kazachenko, A.S. (2023) Synthesis, Empirical and Theoretical Investigations on New Histaminium Bis(Trioxonitrate) Compound. *Molecules*, **28**, Article No. 1931. https://doi.org/10.3390/molecules28041931

[19] Zamisa, S.J. and Omondi, B. (2022) Microwave Assisted Synthesis, Crystal Structure and Hirshfeld Surface Analysis of Some 2-Formimidate-3-Carbonitrile Derivatives Bearing 4H-Pyran and Dihydropyridine Moieties. *Molbank*, **2022**, M1364. https://doi.org/10.3390/M1364

[20] Sukhikh, A., Klyamer, D., Bonegardt, D. and Basova, T. (2023) Octafluoro-Substituted Phthalocyanines of Zinc, Cobalt, and Vanadyl: Single Crystal Structure, Spectral Study and Oriented Thin Films. *International Journal of Molecular Sciences*, **24**, Article No. 2034. https://doi.org/10.3390/ijms24032034

[21] Novoa-Ramírez, C.S., Silva-Becerril, A., Olivera-Venturo, F.L., García-Ramos, J.C., Flores-Alamo, M. and Ruiz-Azuara, L. (2020) N/N Bridge Type and Substituent Effects on Chemical and Crystallographic Properties of Schiff-Base (Salen/Salphen) Niii Complexes. *Crystals*, **10**, Article No. 616. https://doi.org/10.3390/cryst10070616

[22] Asad, M., Arshad, M.N., T.N., M.M. and Asiri, A.M. (2022) Chitosan Catalyzed Novel Piperidinium Dicoumarol: Green Synthesis, X-Ray Diffraction, Hirshfeld Surface and DFT Studies. *Polymers*, **14**, Article No. 1854. https://doi.org/10.3390/polym14091854

[23] Minaeva, V., Karaush-Karmazin, N., Panchenko, O., Minaev, B. and Ågren, H. (2023) Hirshfeld and AIM Analysis of the Methylone Hydrochloride Crystal Structure and Its Impact on the IR Spectrum Combined with DFT Study. *Crystals*, **13**, Article No. 383. https://doi.org/10.3390/cryst13030383

[24] Ruelas-Álvarez, G.Y., Cárdenas-Valenzuela, A.J., Galaviz-Moreno, L.L., Cruz-Enríquez, A., Campos-Gaxiola, J.J., Höpfl, H., Baldenebro-López, J., Vargas-Olvera, E.C., Miranda-Soto, V., García Grajeda, B.A. and Glossman-Mitnik, D. (2022) Four-Coordinate Monoboron Complexes with 8-Hydroxyquinolin-5-Sulfonate: Synthesis, Crystal Structures, Theoretical Studies, and Luminescence Properties. *Crystals*, **12**, Article No. 783. https://doi.org/10.3390/cryst12060783

[25] Zięba, S., Piotrowska, A., Mizera, A., Ławniczak, P., Markiewicz, K.H., Gzella, A., Dubis, A.T. and Łapiński, A. (2021) Spectroscopic and Structural Study of a New Conducting Pyrazolium Salt. *Molecules*, **26**, Article No. 4657. https://doi.org/10.3390/molecules26154657

[26] Zhuang, T.-H., Lin, Y.-M., Lin, H.-W., Guo, Y.-L., Li, Z.-W., Du, K.-Z., Wang, Z.-P. and Huang, X.-Y. (2023) Luminescence Enhancement and Temperature Sensing Properties of Hybrid Bismuth Halides Achieved via Tuning Organic Cations. *Molecules*, **28**, Article No. 2380. https://doi.org/10.3390/molecules28052380

[27] Smarun, A.V., Jevtovic, V. and Ganguly, R. (2020) Synthesis, Structure and Hirshfeld Surface Analysis of Phosphine-Imidazolium Salt. *Molbank*, **2020**, M1141. https://doi.org/10.3390/M1141

[28] Daśko, M., Dołęga, A., Siedzielnik, M., Biernacki, K., Ciupak, O., Rachon, J. and Demkowicz, S. (2021) Novel 1,2,3-Triazole Derivatives as Mimics of Steroidal System—Synthesis, Crystal Structures Determination, Hirshfeld Surfaces Analysis and

Molecular Docking. *Molecules*, **26**, Article No. 4059. https://doi.org/10.3390/molecules26134059

[29] Vassilyeva, O.Y., Buvaylo, E.A., Nesterova, O.V., Sobolev, A.N. and Nesterov, D.S. (2023) New Low-Dimensional Organic-Inorganic Lead Halide Hybrid Systems Directed by Imidazo[1,5-a]pyridinium-Based Cation or Imines: Synthesis, Structures, Non-Covalent Interactions and Optical Properties. *Crystals*, **13**, Article No. 307. https://doi.org/10.3390/cryst13020307

[30] Boraei, A.T.A., Soliman, S.M., Haukka, M., El Tamany, E.S.H., Al-Majid, A.M. and Barakat, A. (2021) X-Ray Single Crystal Structure, Tautomerism Aspect, DFT, NBO, and Hirshfeld Surface Analysis of a New Schiff Bases Based on 4-Amino-5-Indol-2-yl-1,2,4-Triazole-3-Thione Hybrid. *Crystals*, **11**, Article No. 1041. https://doi.org/10.3390/cryst11091041

[31] Collart, A., Zeller, M. and Hillesheim, P.C. (2022) Surface and Void Space Analysis of the Crystal Structures of Two Lithium Bis(pentafluoroethanesulfonyl)imide Salts. *Crystals*, **12**, Article No. 701. https://doi.org/10.3390/cryst12050701

[32] Grudova, M.V., Novikov, A.S., Kubasov, A.S., Khrustalev, V.N., Kirichuk, A.A., Nenajdenko, V.G. and Tskhovrebov, A.G. (2022) Aurophilic Interactions in Cationic Three-Coordinate Gold(I) Bipyridyl/Isocyanide Complex. *Crystals*, **12**, Article No. 613. https://doi.org/10.3390/cryst12050613

[33] Hamlaoui, M., Hamlaoui, I., Damous, M., Belhocine, Y., Sbei, N., Ali, F.A.M., Alghamdi, M.A., Talab, S., Rahali, S. and Merazig, H. (2022) Synthesis of Two Novel Copper(II) Complexes as Potential Inhibitors of HIV-1 Protease Enzyme: Experimental and Theoretical Investigations. *Crystals*, **12**, Article No. 1066. https://doi.org/10.3390/cryst12081066

[34] Shivanna, C., Patil, S.M., Mallikarjunaswamy, C., Ramu, R., Akhileshwari, P., Nagaraju, L.R., Sridhar, M.A., Khanum, S.A., Ranganatha, V.L., Silina, E., Stupin, V. and Achar, R.R. (2022) Synthesis, Characterization, Hirshfeld Surface Analysis, Crystal Structure and Molecular Modeling Studies of 1-(4-(Methoxy(phenyl)methyl)-2-methylphenoxy)butan-2-one Derivative as a Novel α-Glucosidase Inhibitor. *Crystals*, **12**, Article No. 960. https://doi.org/10.3390/cryst12070960

[35] Osman, D.A., Macías, M.A., Al-Wahaibi, L.H., Al-Shaalan, N.H., Zondagh, L.S., Joubert, J., Garcia-Granda, S. and El-Emam, A.A. (2021) Structural Insights and Docking Analysis of Adamantane-Linked 1,2,4-Triazole Derivatives as Potential 11β-HSD1 Inhibitors. *Molecules*, **26**, Article No. 5335. https://doi.org/10.3390/molecules26175335

[36] Abou-Taleb, H.A., Shoman, M.E., Makram, T.S., Abdel-Aleem, J.A. and Abdelkader, H. (2023) Exploration of the Safety and Solubilization, Dissolution, Analgesic Effects of Common Basic Excipients on the NSAID Drug Ketoprofen. *Pharmaceutics*, **15**, Article No. 713. https://doi.org/10.3390/pharmaceutics15020713

[37] Moyano, S., Diosdado, B., San Felices, L., Elduque, A. and Giménez, R. (2021) Structural Diversity of Hydrogen-Bonded 4-Aryl-3,5-Dimethylpyrazoles for Supramolecular Materials. *Materials*, **14**, Article No. 4550. https://doi.org/10.3390/ma14164550

[38] Wattanathana, W., Suetrong, N., Kongsamai, P., Chansaenpak, K., Chuanopparat, N., Hanlumyuang, Y., Kanjanaboos, P. and Wannapaiboon, S. (2021) Crystallographic and Spectroscopic Investigations on Oxidative Coordination in the Heteroleptic Mononuclear Complex of Cerium and Benzoxazine Dimer. *Molecules*, **26**, Article No. 5410. https://doi.org/10.3390/molecules26175410

[39] Zhou, M.-M. and Xiang, D. (2022) Theoretical Prediction of Structures and Properties of 2,4,6-Trinitro-1,3,5-Triazine (TNTA) Green Energetic Materials from DFT

and ReaxFF Molecular Modeling. *Materials*, **15**, Article No. 3873. https://doi.org/10.3390/ma15113873

[40] Standish, K., Zeller, M., Barbosa, A.J. and Hillesheim, P.C. (2022) Examining the Non-Covalent Interactions for Two Polymorphs of a 2,1,3-benzoxadiazole Derivative. *Crystals*, **12**, Article No. 1143. https://doi.org/10.3390/cryst12081143

[41] Rayes, A., Zárate-Roldán, S., Ara, I., Moncer, M., Dege, N., Gimeno, M.C., Ayed, B. and Herrera, R.P. (2021) Single-Crystal-to-Single-Crystal Transformation and Catalytic Properties of New Hybrid Perhalidometallates. *Catalysts*, **11**, Article No. 758. https://doi.org/10.3390/catal11070758

[42] Hirshfeld, F.L. (1977) Bonded-Atom Fragments for Describing Molecular Charge Densities. *Theoretica Chimica Acta*, **44**, 129-138. https://doi.org/10.1007/BF00549096

[43] Psycharis, V., Dermitzaki, D. and Raptopoulou, C.P. (2021) The Use of Hirshfeld Surface Analysis Tools to Study the Intermolecular Interactions in Single Molecule Magnets. *Crystals*, **11**, Article No. 1246. https://doi.org/10.3390/cryst11101246

[44] Spackman, M.A. and Jayatilaka, D. (2009) Hirshfeld Surface Analysis. *CrystEngComm*, **11**, 19-32. https://doi.org/10.1039/B818330A

[45] Carey, J.R., Ma, S.K., Pfister, T.D., Garner, D.K., Kim, H.K., Abramite, J.A., Wang, Z., Guo, Z. and Lu, Y. (2004) A Site-Selective Dual Anchoring Strategy for Artificial Metalloprotein Design. *Journal of the American Chemical Society*, **126**, 10812-10813. https://doi.org/10.1021/ja046908x

[46] Matsuo, T., Imai, C., Yoshida, T., Saito, T., Hayashi, T. and Hirota, S. (2012) Creation of an Artificial Metalloprotein with a Hoveyda-Grubbs Catalyst Moiety through the Intrinsic Inhibition Mechanism of *α*-Chymotrypsin. *Chemical Communications*, **48**, 1662-1664. https://doi.org/10.1039/c2cc16898g

[47] Maglio, O., Nastri, F. and Lombardi, A. (2012) Structural and Functional Aspects of Metal Binding Sites in Natural and Designed Metalloproteins. *Ionic Interactions in Natural and Synthetic Macromolecules*, **11**, 361-450. https://doi.org/10.1002/9781118165850.ch11

[48] Jelsch, C., Ejsmont, K. and Huder, L. (2014) The Enrichment Ratio of Atomic Contacts in Crystals, an Indicator Derived from the Hirshfeld Surface Analysis. *IUCrJ*, **1**, 119-128. https://doi.org/10.1107/S2052252514003327

[49] Groom, C.R., Bruno, I.J., Lightfoot, M.P. and Ward, S.C. (2016) The Cambridge Structural Database. *Acta Crystallographica Section B*, **72**, 171-179. https://doi.org/10.1107/S2052520616003954

[50] Ward, S.C. and Sadiq, G. (2020) Introduction to the Cambridge Structural Database—A Wealth of Knowledge Gained from a Million Structures. *CrystEngComm*, **22**, 7143-7144. https://doi.org/10.1039/D0CE90154G

[51] Turner, M.J., Mckinnon, J.J., Wolff, S.K., Grimwood, D.J., Spackman, P.R., Jayatilaka, D. and Spackman, M.A. (2017) CrystalExplorer17. University of Western Australia, Perth.

[52] Suda, S., Akitsu, T., Onami, Y. and Haraguchi, T. (2021) Orthorhombic Polymorphism of 4-(2-Phenyldiazenyl)-2-[(phenylimino)methyl]phenol. *X-Ray Structure Analysis Online*, **37**, 17-18. https://doi.org/10.2116/xraystruct.37.17

[53] Noor, S., Suda, S., Haraguchi, T., Khatoon, F. and Akitsu, T. (2021) Chiral Crystallization of a Zinc(II) Complex. *Acta Crystallographica Section E*, **77**, 542-546. https://doi.org/10.1107/S2056989021003650

[54] Akitsu, T., Suda, S. and Katsuumi, N. (2021) Beyond the Scope of Each Computational Chemistry. *Edelweiss Chemical Science Journal*, **4**, 25-26.

https://doi.org/10.33805/2641-7383.128

[55] Onami, Y., Siddaraju, B.P., Anilkumar, H.G., Yathirajan, H.S., Haraguchi, T. and Akitsu, T. (2019) (Z)-1-Benzoyl-5-benzylidene-2-hydroxy-4-oxo-4,5-dihydro-1H-pyrrole-3-carbonitrile. *IUCrData*, **4**, x190220. https://doi.org/10.1107/S2414314619002207

[56] Numata, T., Ikenomoto, S. and Akitsu, T. (2016) 4,4'-(1,2-Diazaniumylethane-1,2-diyl) dibenzoate trihydrate. *IUCrData*, **1**, x160252. https://doi.org/10.1107/S2414314616002522

[57] Aritake, Y., Watanabe, Y. and Akitsu, T. (2010) 4-Phenyldiazenyl-2-[(R)-(1-phenylethyl) iminomethyl]phenol. *Acta Crystallographica Section E*, **66**, o749. https://doi.org/10.1107/S1600536810007762

[58] Moriwaki, R., Yagi, S., Haraguchi, T. and Akitsu, T. (2017) 6-[(R)-(2-Hydroxy-1-phenylethyl)aminomethylidene]-4-(2-phenyldiazen-1-yl)cyclohexa-2,4-dien-1-one. *IUCrData*, **2**, x170979. https://doi.org/10.1107/S2414314617009798

[59] Akitsu, T. and Einaga, Y. (2006) A Chiral Photochromic Schiff Base: (R)-4-bromo-2-[(1-phenylethyl)iminomethyl]phenol. *Acta Crystallographica Section E*, **62**, o4315-o4317. https://doi.org/10.1107/S1600536806034891

[60] Miura, Y., Aritake, Y. and Akitsu, T. (2009) A Chiral Photochromic Schiff Base: (R)-4-methoxy-2-[(1-phenylethyl)iminomethyl]phenol. *Acta Crystallographica Section E*, **65**, o2381. https://doi.org/10.1107/S1600536809035557

[61] Akitsu, T. and Einaga, Y. (2003) A Redetermination of bis(N-methylethylenediamine-κ2N,N')bis(perchlorato-κO)copper(II). *Acta Crystallographica Section E*, **59**, m991-m993. https://doi.org/10.1107/S160053680302213X

[62] Akitsu, T. and Einaga, Y. (2004) Bis(5-chloro-N-isopropylsalicyldenaminato-κ2N,O) copper(II). *Acta Crystallographica Section E*, **60**, m436-m438. https://doi.org/10.1107/S1600536804005938

[63] Akitsu, T. and Einaga, Y. (2004) Bis(N-ethyl-ethylenediamine-κ2N,N')copper(II)-hexa-cyano-cobaltate(III)-water (3/2/4): A Two-Dimensional Ladder Structure of a Bimetallic Assembly. *Acta Crystallographica Section E*, **62**, m750-m752. https://doi.org/10.1107/S1600536806008105

[64] Yagi, S., Haraguchi, T. and Akitsu, T. (2004) Crystal Structure of (E)-3-[(2,6-dimethylphenyl) diazenyl]-7-methyl-1H-indazole. *Acta Crystallographica Section E*, **74**, m1421-m1423. https://doi.org/10.1107/S2056989018012483

[65] Moriwaki, R. and Akitsu, T. (2015) Crystal Structure of 2-{(R)-[1-(4-bromophenyl) ethyl]iminomethyl}-4-(phenyldiazenyl)phenol, a Chiral Photochromic Schiff Base. *Acta Crystallographica Section E*, **71**, o886-o887. https://doi.org/10.1107/S2056989015019866

[66] Yamazaki, S., Nishiyama, K., Yagi, S., Haraguchi, T. and Akitsu, T. (2018) Crystal Structure of 3,6-Dihydroxy-4,5-dimethylbenzene-1,2-dicarbaldehyde. *Acta Crystallographica Section E*, **74**, 1424-1426. https://doi.org/10.1107/S2056989018012495

[67] Moon, D., Takase, M., Akitsu, T. and Choi, J.-H. (2017) Crystal Structure of Bis[cis-(1,4,8,11-tetraazacyclotetradecane-κ4N)bis(thiocyanato-κN)chromium(III)] Dichromate Monohydrate from Synchrotron X-Ray Diffraction Data. *Acta Crystallographica Section E*, **73**, 72-75. https://doi.org/10.1107/S2056989016020120

[68] Moon, D., Tanaka, S., Akitsu, T. and Choi, J.-H. (2015) Crystal Structure of Hexakis(urea-κO)chromium(III) Dichromate Bromide Monohydrate from Synchrotron X-Ray Data. *Acta Crystallographica Section E*, **71**, 1336-1339. https://doi.org/10.1107/S2056989015019258

[69] Akitsu, T., Takeuchi, Y. and Einaga, Y. (2004) Racemic 3,5-Dichloro-2-{[(1-phenylethyl)

imino]methyl}phenol. *Acta Crystallographica Section C*, **60**, o801-o802. https://doi.org/10.1107/S0108270104017354

[70] Mahesha, N., Yathirajan, H.S., Furuya, T., Akitsu, T. and Glidewell, C. (2019) The Crystal Structure of 1-(2-Iodobenzoyl)-4-(pyrimidin-2-yl)piperazine: A Three-Dimensional Hydrogen-Bonded Framework, Augmented by π-π Stacking Interactions and I···N Halogen Bonds. *Acta Crystallographica Section E*, **75**, 129-133. https://doi.org/10.1107/S205698901801811X

[71] Akitsu, T. and Einaga, Y. (2005) trans-Bis(2,2-diphenylethylamine-κN)bis(5,5-diphenylhydantoinato-κN3)copper(II) and Its Chloroform Disolvate. *Acta Crystallographica Section C*, **61**, m183-m186. https://doi.org/10.1107/S010827010500209X

[72] Akitsu, T. and Einaga, Y. (2004) trans-Bis(5,5-diphenylhydantoinato)bis(2-phenylethylamine)copper(II). *Acta Crystallographica Section E*, **50**, m524-m526. https://doi.org/10.1107/S1600536804007378

[73] Baldi, P. and Hornik, K. (1989) Neural Networks and Principal Component Analysis: Learning from Examples without Local Minima. *Neural Networks*, **2**, 53-58. https://doi.org/10.1016/0893-6080(89)90014-2

[74] Katsuumi, N., Onami, Y., Pradhan, S., Haraguchi, T. and Akitsu, T. (2020) Crystal Structure and Hirshfeld Surface Analysis of (aqua-κ*O*)(methanol-κ*O*)[*N*-(2-oxidobenzylidene)-threoninato-$\kappa^3 O,N,O'$]copper(II). *Acta Crystallographica Section E*, **76**, 1539-1542. https://doi.org/10.1107/S2056989020011706

[75] Furuya, T., Nakane, D., Kitanishi, K., Katsuumi, N., Tsaturyan, A., Shcherbakov, I. N., Unno, M. and Akitsu, T. (2023) A Novel Hybrid Protein Composed of Superoxide-Dismutase-Active Cu(II) Complex and Lysozyme. *Scientific Reports*, **13**, Article No. 6892. https://doi.org/10.1038/s41598-023-33926-1

[76] Akitsu, T., Kuroda, Y., Suda, S., Furuya, T., Haraguchi, T. and Unno, M. (2021) Weakly Non-Covalent Docking of Amino-Acid Schiff Base Zn(II) Complex to Lysozyme. *Key Engineering Materials*, **888**, 105-110. https://doi.org/10.4028/www.scientific.net/KEM.888.105